Magnetic anisotropy of nanoscale cobalt particles

2004 J. Phys.: Condens. Matter 16 3163

(http://iopscience.iop.org/0953-8984/16/18/017)

INSTITUTE OF PHYSICS PUBLISHING JOURNAL OF PHYSICS: CONDENSED MATTER

J. Phys.: Condens. Matter **16** (2004) 3163–3172 PII: S0953-8984(04)76290-6

Magnetic anisotropy of nanoscale cobalt particles

Yuannan Xie and John A Blackman

Department of Physics, University of Reading, Whiteknights, PO Box 220, Reading RG6 6AF, UK

Received 16 February 2004
Published 23 April 2004
Online at stacks.iop.org/JPhysCM/16/3163
DOI: 10.1088/0953-8984/16/18/017

Abstract

We report calculations of the magnetic anisotropy energy (MAE) of cobalt nanoparticles in the size range 300–1000 atoms. The MAE is expressed in terms of shell-resolved contributions from different parts of the cluster. The net anisotropy is a delicate balance between contributions from the interior and the surface of the cluster that generally have opposite signs. We study closed shell structures for which the MAE is fourth order in the spin–orbit coupling, and clusters for which additional layers have been added to the facets, inducing uniaxial anisotropy. Both Co and Cu facet additions are considered. The relation of the results to experimental work is discussed.

1. Introduction

Single domain magnetic nanoclusters are of considerable current interest. This interest has been spurred on because of their potential as high density data storage materials. The ability to control the properties of these systems is rapidly developing, but there are a number of issues of fundamental physics that still require investigation. Crucial among these is the magnetic anisotropy energy (MAE) [1–4], which determines the low temperature orientation of the magnetization with respect to the structure of the system. It is important to take the MAE into account to understand the superparamagnetic behaviour of free clusters in a magnetic field [5].

Most of the experimental studies [1–3] on nanosized grains have been carried out on large assemblies of particles. It is found that the anisotropy of a particle exceeds the bulk value, and this excess has been correlated with the enhanced orbital moment of the atoms near the surface. The dependence of the effective anisotropy on particle size is measured, but full details about the MAE are inaccessible because one is studying an ensemble average rather than the behaviour of a single particle.

An important recent advance is the development of a micro-SQUID system to measure the anisotropy of a single particle. Values of the second and fourth order anisotropy constants have been obtained for a 3 nm cobalt cluster embedded in niobium. The experimental results [4] were interpreted in terms of a model nanocluster comprising a truncated octahedron of about

1000 atoms with added planes of atoms on some facets to reflect the known growth modes of such clusters.

There have been a number of calculations [6, 7] of the MAE of small metallic clusters. Complicated behaviour is found and this has been studied as a function of the particle size and morphology. The largest cluster to date on which MAE calculations have been performed based on a model of the electronic structure contained 79 atoms [7].

As first discussed by van Vleck [8], magnetocrystalline anisotropy originates from spin–orbit interaction. It has been found that the orbital moment and the magnitude of MAE from first-principles calculations [9, 10] within the local spin-density approximation (LSDA) are too small, and that the predicted easy axis for fcc Ni is wrong. The LSDA can be improved [10] by adding corrections of Brooks' orbital polarization term [11] which mimics Hund's second rule. It has been shown also that the MAEs calculated from a tight-binding (TB) model fitted to *ab initio* band structures can reach the same accuracy as those predicted from the *ab initio* calculations, and the inclusion of orbital polarization is equivalent to increasing the effective spin–orbit coupling parameters [12]. Problems still remain with fcc Ni [10, 12], but the procedure is secure for Co, the material of interest in the current paper.

We have performed calculations on the MAE of fcc cobalt clusters in the size range 300–1000 atoms. To our knowledge this work is the first theoretical study of the MAE of particles whose size approaches that of current experimental interest.

2. Method

We use a self-consistent TB methodology in which a minimal orthogonal basis set containing s, p and d orbitals is used. This was employed earlier [13, 14] to calculate the spin-magnetization of embedded Fe and Co particles, and the parameters for Co are given there [14]. Spin–orbit coupling in the usual single-site form is added to the tight-binding Hamiltonian with the coupling parameter 88 meV for d-orbitals [15], which is larger than those used in LSDA calculations at the d-band centre (77 meV) and at the Fermi energy (85 meV) [9]. The orbital moment of the bulk atoms predicted from our TB calculations is about 0.11 μ_B/atom [14], in good agreement with that predicted from LSDA calculation with orbital polarization correction [10].

The TB method [14] implicitly assumes a spherical potential around each atom, which should not significantly affect the accuracy of the MAE, because the major contribution of the spin–orbit coupling occurs in the inner atom region, where the potential is approximately spherical [9]. In contrast to the many calculations that employ perturbation theory and the force theorem [16], we diagonalize the tight-binding Hamiltonian exactly. Due to the smallness of the MAE, special care needs to be taken concerning k-space integration for bulks or films [17, 18]. In our cluster calculations, *all* eigenstates are included, and the numerical accuracy of total energy difference calculations is better than 0.1 μeV. Due to the redistribution of spin-density between geometrically equivalent sites, it is important to perform the calculations self-consistently. All clusters considered have some symmetry, albeit a lower one than in the absence of the spin–orbit interaction. Use of the symmetry adapted basis of the double point group in the determination of the MAE reduces the size of the calculation to a manageable level.

In the form of clusters, Co takes either the fcc or icosahedral structure, but when deposited on a surface, the nanoparticles form mainly truncated octahedra [4, 19]. The cuboctahedron, an octahedron truncated by a cube, can have two forms [20], one with triangular (111) facets (T-*cubo*), the other with hexagonal (111) facets (H-*cubo*). The T-*cubo* has the geometrical closed shell sequence 13, 55, 147, 309, 561, 923, while for H-*cubo* it is 38, 201, 586, 1289.

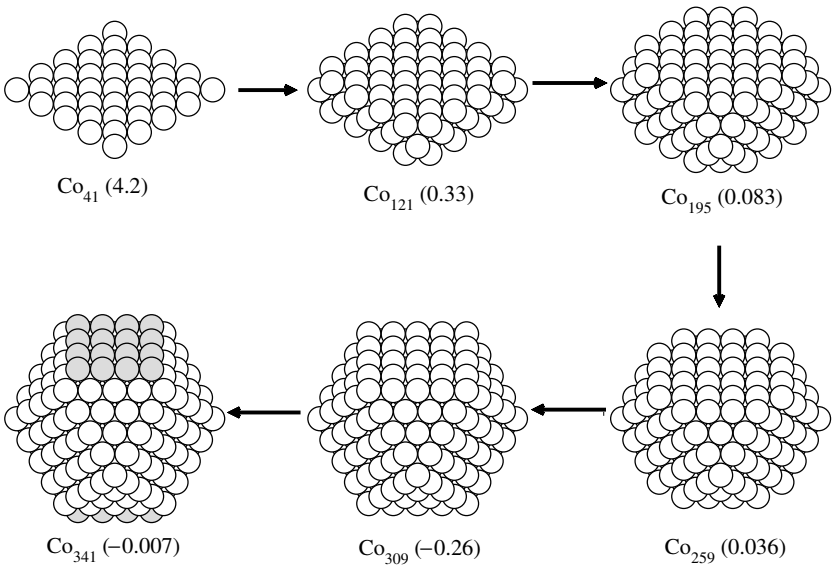

Figure 1. Examples of 1, 3, 5, 7, 9, 11 layer structures of Co atoms. The Co_{309} cluster has O_h symmetry. Shaded atoms in Co_{341} indicate atoms added to facets of Co_{309}. Figures in parentheses show the MAE: $E_{001}-E_{100}$ in units of meV/atom for the 41, 121, 195, 259 and 341 atom clusters, and $E_{111}-E_{001}$ in units of μeV/atom for Co_{309}.

It is believed that the growth mode of clusters between filled geometric shell configurations is via sequential filling of the adjacent facets [4, 19, 20].

The results are presented as follows. First we consider finite layers and slabs to provide an overview and to connect to other results in the literature. We then examine some clusters with full cubic symmetry. This will give useful insight into the behaviour of the MAE in clusters, and also serves as a basis from which to explore the effect on the MAE of facet filling, which is the main purpose of this paper.

3. Results

3.1. Layers to clusters

We begin by making a connection with established results. Model closed shell clusters of the T-*cubo* type can be built from a series of (001) layers, starting with a central one and then adding successively pairs of layers, one on either side, until the complete clusters are formed. This is illustrated in figure 1, where a 309 atom cluster is built up successively through 1, 3, 5, 7 layer structures starting with a single 41 atom layer. The final 341 atom cluster provides an example of additional facets added to the closed shell 309 atom cluster. The MAE has been calculated at each stage of the construction. The values found for $E_{001}-E_{100}$ for the 41, 121, 195, 259 and 341 atom clusters are indicated on the figure in units of meV/atom. The 309 atom cluster, of course, has cubic symmetry and the (001) and (100) directions are equivalent. In this case, the value of $E_{111}-E_{001}$ is shown in units of μeV/atom. In-plane alignment is preferred for the 41, 121, 195 and 259 atom structures, while alignment perpendicular to the added facets is obtained for Co_{341}. The MAE of an infinite monolayer predicted by *ab initio* calculations [21, 22] is of the order of 1 meV/atom, with in-plane easy axis. Our result of 4.2 meV/atom for the single 41 atom layer is a somewhat higher than that for an infinite plane, as one would expect. For

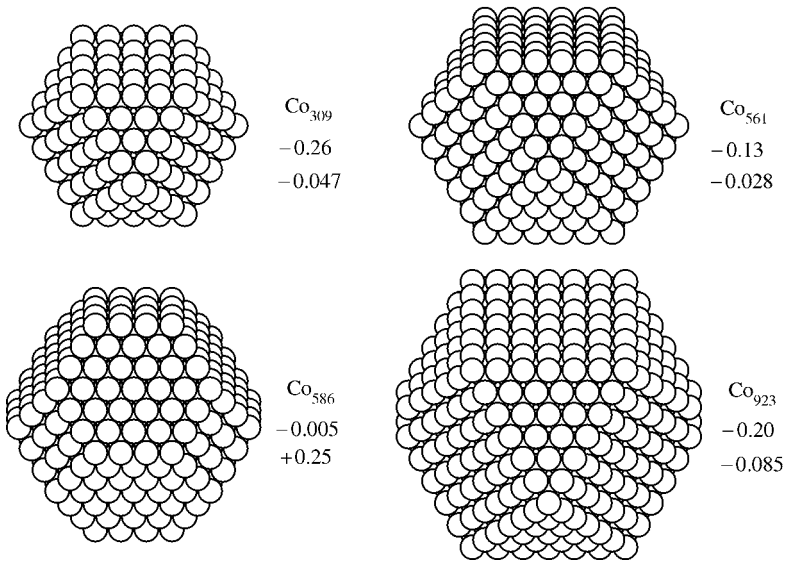

Figure 2. Clusters with T-*cubo* (Co_{309}, Co_{561}, Co_{923}) and H-*cubo* (Co_{586}) structures. The MAE values (in μeV/atom) of E_{111}–E_{001} and E_{110}–E_{001} are indicated under the cluster symbols.

slabs, a typical figure is about 0.3 meV/unit cell [16] fairly independent of the slab thickness. Our values for the MAE for the three and five layer structures are a little higher than those for the infinite slabs, and become smaller at seven layers as the cubic symmetry 309 cluster is approached. Co_{309} has the same O_h symmetry as the bulk material and we find a similar (111) easy axis. The closed-shell structures are discussed in the following section.

3.2. O_h symmetry clusters

We now consider four closed shell clusters, three of the T-*cubo* type with 309 (as above), 561 and 923 atoms, and a 586-atom H-*cubo* structure, as illustrated in figure 2. The calculated MAEs are also displayed in the figure. In each case the (111) orientation is the easy axis as in bulk, but the MAE is significantly smaller in value than that of the bulk ($\sim$1 μeV/atom) [10, 18], and markedly so for the 586 atom cluster. The T-*cubo* structures behave in the same way as the bulk in the sense that $E_{111} < E_{110} < E_{001}$. However, for the H-*cubo* Co_{586} cluster, while the easy axis is again (111), the hard axis is (110). The MAE is quite sensitive to the geometrical shape.

The MAEs of magnetic films are often analysed in terms of surface/interface and bulk anisotropies [1, 3, 23]. We prefer to express the behaviour in terms of shell-resolved contributions. We can derive the shell-resolved contribution to the MAE from local contribution to the total energy

$$E_\delta^i = \sum_\sigma \int_{-\infty}^{\varepsilon_F} \varepsilon \rho_{i\sigma}(\varepsilon)\, \mathrm{d}\varepsilon - E_{\mathrm{dc}}^i, \tag{1}$$

where $\rho_{i\sigma}(\varepsilon)$ is the local density of states of spin σ at site i and E_{dc}^i the double counting correction at site i. δ refers to the magnetization direction.

We compare the contributions to E_{111}–E_{001} for the 561 and 586 atom clusters in figure 3. The total contributions from different groups of sites are shown. The breakdown for the surface sites is by square and triangular (or hexagonal) faces, edges and vertices. For the inner parts

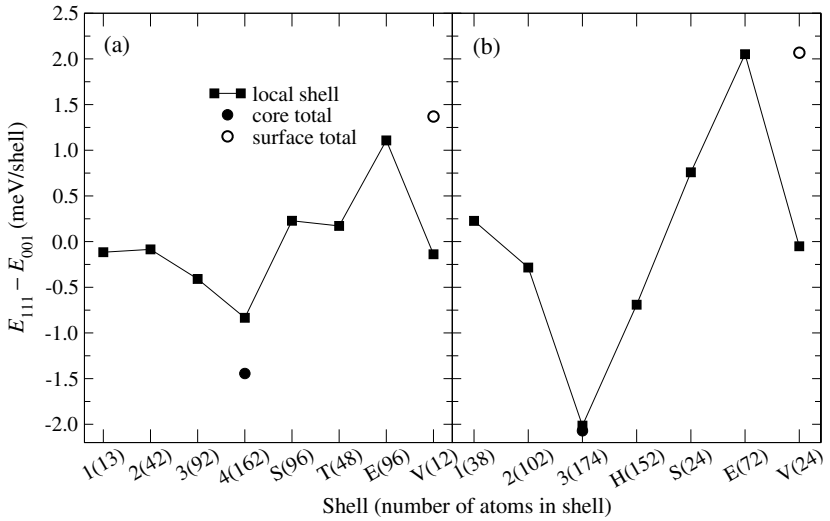

Figure 3. Shell-resolved contributions (square symbols) to the MAE for (a) Co_{561} and (b) Co_{586}. The contribution from the central atom of Co_{561} is included in the first shell. The shells of Co_{586} are defined as the central group of 38 atoms, the group of 174 atoms that are neighbours to surface atoms, and the 102 atoms lying between the previous two groups. The number of atoms in a shell is indicated in the brackets. The surface layer is decomposed into groups of atoms on the square facets (S), atoms on the triangular/hexagonal facets (T/H), atoms on the edges (E), and atoms at the vertices (V). The closed circle is the total contribution from the interior and the open circle is the total surface contribution.

of the cluster, we divide the sites into a central core, atoms that are nearest neighbours to the surface, and those that are between the two groups. The numbers of atoms of each type are shown in the figures. The 561 atom T-*cubo* cluster can be constructed shell by shell, and for this case the labelling is by shell.

Considering first the 561 atom cluster and figure 3(a), we see that, apart from the small component from the vertices, the surface contribution is positive, while that from the inner atoms is negative, with the dominant contributions coming from the edge atoms and from the shell of atoms adjacent to those on the surface. The total contributions to $E_{111}-E_{001}$ from the interior and the surface are -1.444 and +1.369 meV, respectively, giving a net MAE for the cluster of -0.075 meV (or -0.13 μeV/atom as in figure 2). On a per atom basis, the interior and surface contributions are, respectively, -4.7 and 5.4 μeV/atom. The dominant contribution from the shell adjacent to the surface is simply a reflection of the large number of atoms (162) in this group, while the edge component has an above average magnitude of 11.5 μeV/atom.

Qualitatively similar behaviour is seen in the plot for the 586 atom cluster in figure 3(b), with contributions of -2.071 and +2.068 meV, respectively, from the interior and the surface, giving a net MAE of -0.003 meV (or -0.005 μeV/atom as in figure 2). Edge atoms and those adjacent to the surface again dominate, but now the contributions from the two types of faces have opposite sign.

The calculations have been performed with the lattice spacing fixed at the bulk value. In practice there will be relaxation of the lattice, so there could be a significant shift from the values of MAE that we have predicted. However the partial cancellation between positive and negative contributions will still apply and so the precise value will be extremely sensitive to the details of the cluster morphology. The clusters we have looked at are still quite small (<3 nm in diameter).

Table 1. MAEs in meV for N atom clusters with planes of n atoms added to 001 and $00\bar{1}$ facets. The anisotropy constants in μeV/atom are defined in equation (2). The number of atoms in a cluster is $N + 2n$. The results with the magnetic dipole interaction included are given in brackets.

N/n	E_{100}–E_{001}	E_{110}–E_{001}	K_1	K_4
309/16	2.2 (4.0)	1.8 (3.5)	−6.5 (−11.7)	−4.7 (−5.8)
561/25	22.2 (24.7)	21.3 (23.8)	−36.3 (−40.4)	−5.9 (−5.9)
586/9	7.2 (8.6)	6.7 (8.2)	−11.9 (−14.2)	−3.3 (−2.6)

As the size increases we expect that the contribution to the MAE from the surface will become proportionally smaller than that from the interior, the degree of cancellation between the two contributions will decrease, and eventually the MAE will approach its bulk value.

Analogous behaviour has also been noted in thin film systems [24]. In that case, of course, the number of atoms in each layer is the same, while in the systems studied here the number in each shell in addition to the contributions per atom is essential in determining the balance between positive and negative contributions.

In the analysis of experimental data on cobalt nanoparticles, Jamet *et al* [4] note that the fourth order MAE that they obtain (0.23 μeV/atom for a ∼1000-atom cluster) is much smaller than that of bulk fcc Co. Their observation occurs in the analysis of a lower symmetry cluster than the ones we are dealing with in this section (they calculate a second and fourth order MAE). However their observation is an interesting one in the context of our results on high symmetry nanoclusters, where we demonstrate that the net fourth order MAE can be expected to be smaller than that of the bulk, whereas intuitively one might expect an enhancement due to the presence of the surface.

3.3. Lower symmetry clusters

Having gained some insight into the behaviour by looking at some closed shell cases, we will now examine systems in which an additional layer of atoms has been added to the facets of the cuboctahedra to give departures from O_h geometrical symmetry.

We consider two types of addition patterns, and retain some symmetry to facilitate the calculation: (a) the basic cluster has an added layer over two opposite square faces; (b) the basic cluster has an additional layer over four hexagonal or triangular faces (111), $(1\bar{1}1)$, $(\bar{1}\bar{1}\bar{1})$ and $(\bar{1}1\bar{1})$. The clusters studied are illustrated in figure 4. The clusters are labelled N/n indicating the number, N, of atoms in the basic cluster and the number, n, added per facet.

The energies are calculated for three magnetization orientations and the results displayed for six cluster configurations in tables 1 and 2. The anisotropy constants K are defined by equations that relate the energy to the direction cosines, α, of the magnetization vector (x, y, z correspond to 100, 010, 001), with the form of the equations being determined by symmetry. The equations used are, for the square face additions,

$$E = K_1\alpha_z^2 + K_4\alpha_x^2\alpha_y^2 \tag{2}$$

and

$$E = K_1\alpha_z\alpha_x + K_2\alpha_y^2 \tag{3}$$

for triangular and hexagonal face additions. For these low symmetry clusters, the magnetic dipole interaction contributes to the MAEs [15]. The MAEs with magnetic dipole interaction included are also presented in the tables. The shape anisotropy [15] is calculated by summing over all pairs of dipole interactions within a single cluster. It can be seen that for most cases considered in our calculations, the MAEs are mainly determined from spin–orbit coupling.

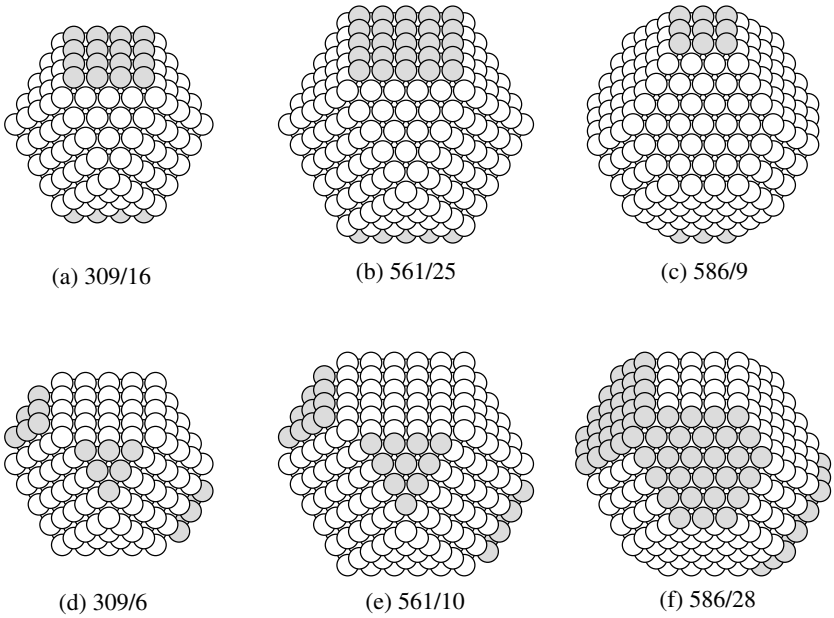

Figure 4. Clusters with layers of atoms added to two square facets (a)–(c) or added to four triangular/hexagonal facets (d)–(f). The notation N/n indicates an O_h symmetry cluster of size N with n additional atoms per facet. The open symbols represent Co atoms. Shaded spheres represent either Co or Cu.

Table 2. MAEs in meV for N atom clusters with n atoms added to 111 and $1\bar{1}1$ facets and the same number to the $\bar{1}\bar{1}\bar{1}$ and $\bar{1}1\bar{1}$ facets. The anisotropy constants in μeV/atom are defined in equation (3). The number of atoms in a cluster is $N + 4n$. The results with the magnetic dipole interaction included are given in brackets.

N/n	$E_{010}-E_{101}$	$E_{10\bar{1}}-E_{101}$	K_1	K_2
309/6	7.5 (8.2)	6.3 (7.7)	−18.9 (−23.1)	13.1 (13.1)
561/10	10.7 (11.8)	16.4 (18.6)	−27.3 (−30.9)	4.2 (4.2)
586/28	18.3 (20.3)	20.6 (23.1)	−29.5 (−33.1)	11.5 (12.5)

The anisotropy constants, K_1 and K_2, that appear in tables 1 and 2 have a magnitude in the range 4–37 μeV/atom. This is equivalent in the commonly used experimental units to 0.6–5.3 $\times$ 10^5 J m^{-3}. Jamet *et al* [4] used two second order anisotropy constants in fitting their experimental results, which they evaluate at 2.2 $\times$ 10^5 and 0.9 $\times$ 10^5 J m^{-3}, which fit precisely within the range we obtain. There has also been a recent study [3] of an assembly of Co clusters between 25 and 7000 atoms embedded in Al_2O_3. This work shows that the effective anisotropy constant $K_{\rm eff}$ is enhanced with respect to bulk value and decreases from 24 to 5 $\times$ 10^5 J m^{-3} with increasing cluster size ($K_{\rm eff} \sim 7 \times 10^5$ J m^{-3} for $N \sim 1000$).

Of course, one has to qualify claims of good agreement between theory and experiment for these systems. The clusters examined experimentally by Jamet *et al* [4] were embedded in Nb; there is an issue about magnetically dead layers [4, 25], and the model of facet filling is slightly different from ours [4]. Similarly, in the other experimental work cited [3], the clusters are also embedded, in that case in an oxide matrix. However, it is interesting to note that in all cases, the MAE obtained for clusters in the 2–3 nm diameter range is between 10^5

Table 3. MAEs in meV for two of the cluster configurations from table 1. The effect of added layers of Co and Cu are compared.

	$E_{100}-E_{001}$		$E_{110}-E_{001}$	
N/n	Co	Cu	Co	Cu
561/25	22.2	11.9	21.3	10.9
586/9	7.2	5.8	6.7	5.4

Table 4. MAEs in meV for two of the cluster configurations from table 2. The effect of added layers of Co and Cu are compared.

	$E_{010}-E_{101}$		$E_{10\bar{1}}-E_{101}$	
N/n	Co	Cu	Co	Cu
561/10	10.7	5.5	16.4	7.6
586/28	18.3	4.7	20.6	12.4

and 10^6 J m^{-3}. It may indicate that the value of the MAE of Co nanoclusters of this type is relatively insensitive to the environmental conditions.

To investigate this point further we have calculated the MAE of clusters in which Cu atoms have been added to the facets of closed shell Co clusters instead of the Co additions treated previously. We consider the (b), (c), (e) and (f) clusters of figure 4. The anisotropy energies of the clusters with Co and Cu facet additions are compared in tables 3 and 4. Except for one case, $E_{010}-E_{101}$ for the 586/28 cluster, all the energies are within a factor of two of each other.

Having been alerted by the behaviour of the regular clusters to the delicate balance between positive and negative contributions to the MAE, we have done a similar analysis here. The 561/25 cluster is used for illustration. The contributions from the various shells of the basic cluster and the facet additions are shown in figure 5(a) for the Co additions and in figure 5(b) for the Cu additions.

For the Co additions we see again contributions of opposite signs to the MAE. In this case we observe a positive contribution from the basic 561 atom cluster and a negative contribution from the layers added to two facets. When the added atoms are Cu, they contribute negligibly to the MAE; the induced magnetization on Cu is very small. Most of the MAE is contributed by the outer shell of the basic 561 atom cluster, as can be seen in figure 5(b). For the clusters as a whole there is only a factor of about two between the MAEs resulting from Co or Cu additions.

4. Conclusions

We have calculated the MAEs of metallic Co clusters whose diameters are in the range of particular experimental interest, 2–3 nm. As a preliminary, finite layers and slabs were studied to make contact with other work in the literature on infinite monolayer and slab calculations. Closed shell configurations were then examined, and it was shown that generally the MAE comprises positive and negative components. There is a delicate balance between the two, and this leads to an anisotropy that is actually smaller than the bulk value. Because the MAE is fourth order in the spin–orbit coupling and very small, one would not claim high quantitative precision to these results, but the general behaviour found is very instructive.

Greater quantitative reliability can be expected with departures from O_h symmetry, and an anisotropy that is second order in the spin–orbit coupling. If the atoms added to the facets

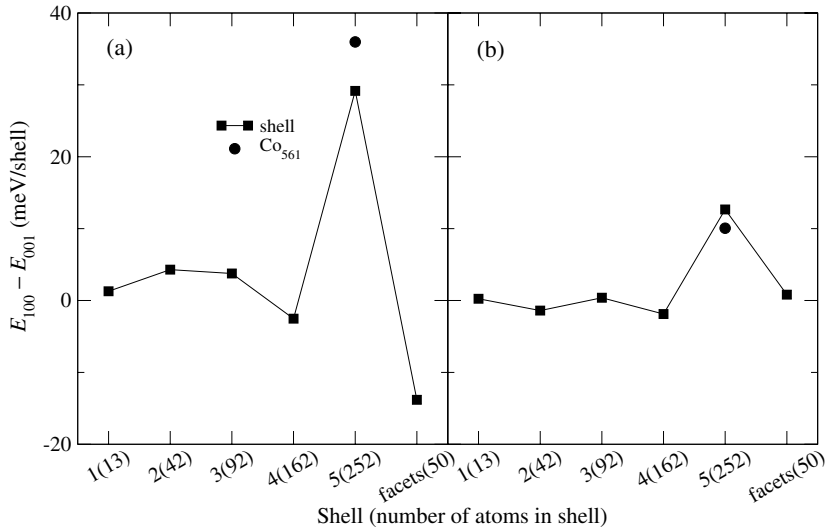

Figure 5. Shell-resolved and added layer contributions to the MAE for the 561/25 cluster, where the added atoms are (a) Co and (b) Cu. The shell labelling is as in figure 3(a). The closed circle shows the total contribution from the Co_{561} core.

are Co, as in the basic cluster, then we again get a balance between positive and negative contributions, but clearly not so delicate as in the high symmetry clusters. A comparison was made between the MAEs obtained with Co or Cu additions. Generally they were the same within a factor of about two. Clearly, the MAE of a cluster is mainly determined by its global geometrical symmetry. If the existence of a disordered surface layer can result in an obvious departure from O_h symmetry, we believe that the MAE will be much higher than that of bulk fcc Co.

All calculations reported in this paper were done at interatomic spacings fixed at the bulk Co value. Work done by others on small clusters indicate a sensitivity of the MAE to lattice relaxation, and it would be interesting to examine the effect of relaxation on the larger clusters studied here. However, it may be that values of MAE are more robust for these larger systems. We have already noted that replacing additional layers of Co atoms by Cu yields an MAE that differs by a factor seldom more than two. Reference to experimental results was also made. Interestingly both theory and experiment yields values of anisotropy inside the range 10^5–10^6 J m^{-3} even though the details of the systems studied experimentally differed markedly from each other and from our theoretical model.

Acknowledgments

This work was supported by the EC through the AMMARE project (Contract No G5RD-CT-2001-00478) under the Competitive and Sustainable Growth Programme. Useful conversations with Alain Pérez are acknowledged.

References

[1] Bødker F, Mørup S and Linderoth S 1994 *Phys. Rev. Lett.* **72** 282
[2] Chen J P, Sorensen C M, Klabude K J and Hadjipanayis G C 1995 *Phys. Rev.* B **51** 11527

[3] Luis F, Torres J M, García L M, Bartolomé J, Stankiewicz J, Petroff F, Fettar F, Maurice J-L and Vaurès A 2002 *Phys. Rev.* B **65** 094409
[4] Jamet M, Wernsdorfer W, Thirion C, Mailly D, Dupuis V, Mélinon P and Pérez A 2001 *Phys. Rev. Lett.* **86** 4676
[5] Xie Y and Blackman J A 2003 *Appl. Phys. Lett.* **82** 1446
[6] Pastor G M, Dorantes-Dávila J, Pick S and Dreyssé H 1995 *Phys. Rev. Lett.* **75** 326
[7] Guirado-López R 2001 *Phys. Rev.* B **63** 174420
[8] Van Vleck J 1937 *Phys. Rev.* **52** 1178
[9] Daalderop G H O, Kelly P J and Schuurmans M F H 1990 *Phys. Rev.* B **41** 11919
[10] Trygg J, Johansson B, Eriksson O and Wills J M 1995 *Phys. Rev. Lett.* **75** 2871
[11] Brooks M S S 1985 *Physica* B **130** 6
[12] Schneider G and Jansen H J F 2000 *J. Appl. Phys.* **87** 5875
[13] Xie Y and Blackman J A 2002 *Phys. Rev.* B **66** 85410
[14] Xie Y and Blackman J A 2002 *Phys. Rev.* B **66** 155417
[15] Bruno P 1993 *Magnetismus von Festkörpern und Grenzflächen* ed P H Dederichs, P Grünberg and W Zinn (Jülich: KFA Jülich) pp 24.1–.28
[16] Cinal M, Edwards D M and Mathon J 1994 *Phys. Rev.* B **50** 3754
[17] Wang D, Wu R and Freeman A J 1993 *Phys. Rev. Lett.* **70** 869
[18] Halilov S V, Perlov A Y, Oppeneer P M, Yaresko A N and Antonov V N 1998 *Phys. Rev.* B **57** 9557
[19] Tuaillon J, Dupuis V, Melinon P, Prevel B, Treilleux M, Pérez A, Pellarin M, Vialle J L and Broyer M 1997 *Phil. Mag.* A **76** 493
[20] Martin T P 1996 *Phys. Rep.* **273** 199 and references therein
[21] Daalderop G H O, Kelly P J and Schuurmans M F H 1994 *Phys. Rev.* **50** 9989
[22] Gay J G and Richter R 1987 *J. Appl. Phys.* **61** 3362
[23] Chuang D S, Ballentine C A and O'Handley R C 1994 *Phys. Rev.* B **49** 15084
[24] Henk J, Niklasson A M N and Johansson B 1999 *Phys. Rev.* B **59** 9332
[25] Pick S, Turek I and Dreyssé H 2002 *Solid State Commun.* **124** 21